

Novel dinuclear iron(0) complexes from α,β -unsaturated ketones β -positioned with sulfide and sulfoxide groups

M. Carmen Ortega-Alfaro, Néstor Hernández, Ismael Cerna, José G. López-Cortés, Elizabeth Gómez, Ruben A. Toscano, Cecilio Alvarez-Toledano *

Instituto de Química UNAM, Circuito Exterior, Ciudad Universitaria, Coyoacán, C.P. 04510 México, D.F.

Received 7 October 2003; accepted 1 December 2003

Abstract

The reaction of $\text{Fe}_2(\text{CO})_9$ with α,β -unsaturated ketones analogues containing β -positioned sulfoxide group **2a–2d** afforded dinuclear Fe(0) complexes **3a–3d** and **5** which were characterized by IR, mass spectrometry, ^1H and ^{13}C NMR spectroscopy, the structures of **3a**, **3c** and **5** were established by X-ray diffraction analysis.

© 2003 Elsevier B.V. All rights reserved.

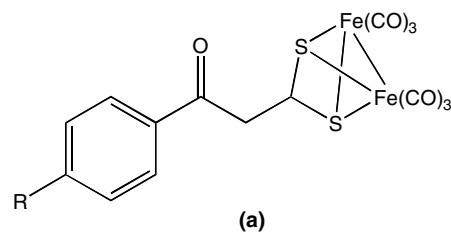
Keywords: Sulfoxides; Dinuclear Fe(0) complexes; X-ray diffraction

1. Introduction

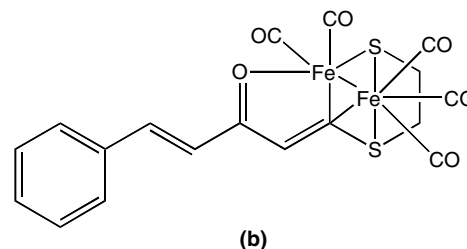
In recent years, Fe(0) complexes have received much attraction owing to their structural diversity and widespread application in organic and organometallic chemistry. Among these interesting compounds especial attention has been aimed to the study of Fe(0) vinylketone complexes and their transformation into vinylketene Fe(0) complexes as well [1–4].

Our interest in the iron chemistry led us to synthesize new mono and dinuclear Fe(0) complexes which have been prepared by reaction of α,β -unsaturated ketones analogues containing β -positioned heteroatoms with $\text{Fe}_2(\text{CO})_9$ [5–8]. In connection with these studies, we have reported that α,β -unsaturated ligands possessing the dithiol group reacts with diiron nonacarbonyl affording dinuclear complexes (**a**) [6]. However, ligands which contain an additional conjugated double bond such as 4-phenyl-1-(1,3-dithiolane-2-ylidene)-3*E*-butenone gives the dinuclear Fe(0) complex (**b**) in which an iron atom was inserted into C–S bond by aperture of the

dithiolane ring, additionally, the coordination of carbonyl ketone group is also observed [7].



R= *o*-OCH₃, *m*-OCH₃, *p*-OCH₃



In continuing with our studies, we herein report the synthesis of α,β -unsaturated ketones with sulfoxide group in β -position **2a–2d**, which were reacted with $\text{Fe}_2(\text{CO})_9$ affording to dinuclear Fe(0) complexes **3a–3d** exhibiting novel coordination patterns.

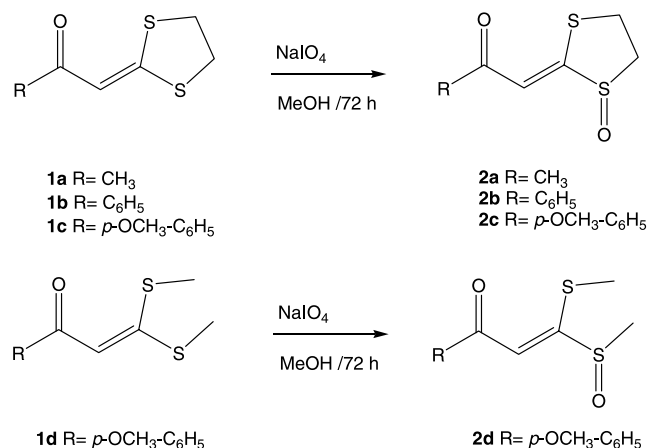
* Corresponding author. Fax: +52-5556162217.

E-mail address: cecilio@servidor.unam.mx (C. Alvarez-Toledano).

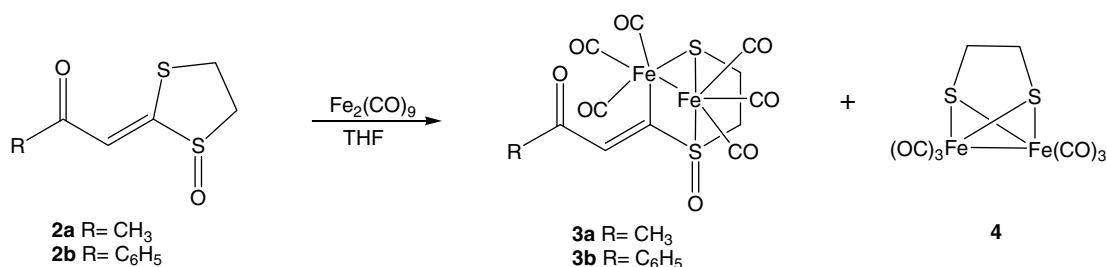
2. Results and discussion

The sulfoxides **2a–2d** were conveniently prepared in 25–38% yield by selective oxidation of 1-(1,3-dithiolane-2-yliden) acetone derivatives **1a–1d** [9,10] using sodium periodate as oxidizing agent [11] (Scheme 1). All compounds displayed in the IR spectrum the absorption band for the sulfoxide group around 1045 cm^{-1} . The NMR data show that the reactions for obtaining compounds **2a–2c** proceed with regio- and stereoselectivity affording exclusively the *E* isomer. The ^1H NMR spectra of compounds **2a–2c** showed four multiplets from 3.0 to 3.9 ppm for methylene groups. In addition, the ^{13}C NMR spectrum for **2a–2c** shows that the carbons bonded to the sulfoxide are shifted upfield ($\delta \sim 20$) with respect to the carbon born by the sulfide. In contrast, no stereoselectivity was observed for the reaction with **1d**, which under the same conditions yielded a mixture of compounds. From the mixture only **2d** could be isolated and purified by chromatography on alumina, which was evidenced by ^1H and ^{13}C NMR spectra. This fact can be explained in terms of a strong electronic interaction between p and d orbital of oxygen and sulfur atoms through the conjugated system [12].

The reaction of **2a**, **2b** and $\text{Fe}_2(\text{CO})_9$ in anhydrous THF (Scheme 2) led to the formation of complexes **3a**,

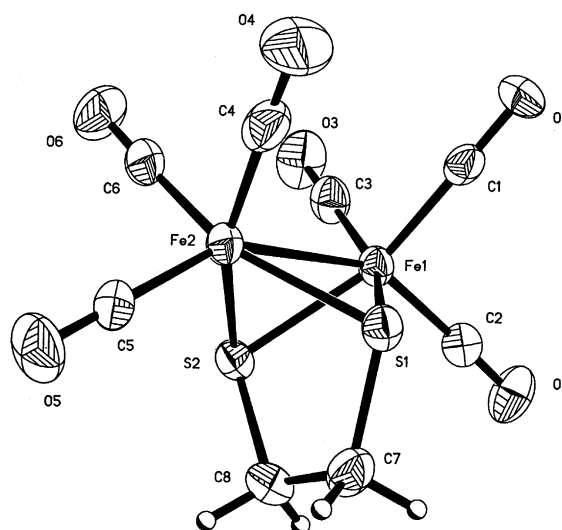


Scheme 1.



Scheme 2.

3b and **4** which were isolated by silica-gel chromatography, after usual workup. The IR spectra of **3a** and **3b** show three absorption bands typical of (M–CO) in the region of $2089\text{--}1954\text{ cm}^{-1}$. Mass spectrometry show peaks at $m/z = 428$ and 490 which correspond to $\text{RCOCH}=\text{C}(\text{S}-\text{CH}_2-\text{CH}_2-\text{S})\text{Fe}_2(\text{CO})_5$ moiety [$M^+ - 28$] for **3a** and **3b**, respectively, in addition, the peaks corresponding to successive loss of five CO groups were also detected. These data suggest the formation of a dinuclear complex. The ^1H NMR spectra of **3a** and **3b** exhibit singlets at 7.35 and 8.15 ppm, respectively, which were assigned to vinylic protons. Furthermore, signals for the methylene groups of **3a** and **3b** appeared in the region of 2.62–3.58 ppm, which are slightly shifted to high frequency with respect to **2a–2b**. The ^{13}C NMR spectra of **3a**, **3b** show that the carbon attached to the sulfoxide are shifted to higher frequencies ($\delta = 10$) compared with **2a** and **2b**, this behavior could be attributed to the presence of iron. Signals at 206.6 and 190.8 ppm were displayed for M–CO group. Complex **4** was obtained as byproduct of the reaction in a very low yield (2%) as reported elsewhere [7,13].

Fig. 1. ORTEP drawing of compound **4**. Thermal ellipsoids at 30% probability level.

The structure of **4** (Fig. 1) was established by X-ray diffraction analysis as a second (monoclinic) polymorph of the structure reported by Hughes et al. [14]. This simpler polymorph has $Z' = 1$ in $P2_1/n$ showing no differences in the geometrical parameters with respect to those found in the $P\bar{1}$ polymorph with $Z' = 2$ (Table 1).

It is important to mention that the reaction of **2c** with $\text{Fe}_2(\text{CO})_9$ under identical conditions led to the formation of complexes **3c**, **4** and **5** (Scheme 3). The IR spectrum of **3c** and **5**, shows M–CO absorption bands in the range 2081–1961 cm^{-1} . The Mass spectrometry spectrum of **3c** displayed a peak $m/z = 492$ corresponding to the fragment $[\text{M}^+ - 2\text{CO}]$ and peaks for successive loss of four CO ligands indicating that complex **3c** possesses a similar structure to those of **3a** and **3b**. On the other hand, complex **5** exhibits the peak

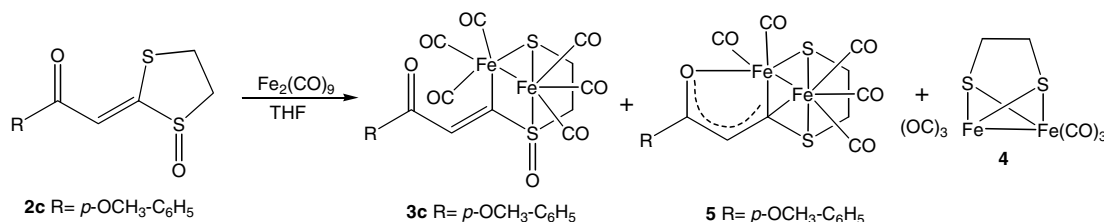
$m/z = 504$, which correspond to the molecular weight of a reduced dinuclear species containing five metal carbonyl groups. Interestingly, the complex **5** could explain the formation of **4**, however, this intermediate **5** was not detected in the previous reactions. This fact evidences the well-known reductive capacity of $\text{Fe}_2(\text{CO})_9$ [15]. ^1H NMR data show a singlet at 8.12 and 7.45 ppm for vinylic proton of **3c** and **5**, respectively, which are slightly shifted to high frequency with respect to free ligand. This behavior is also observed in ^{13}C -NMR spectra for OSCH_2 , CFeSO and CHCFeSO . The structures of **3a** and **3c** and **5** were confirmed by X-ray diffraction analysis. Compounds **3a** and **3c** (Figs. 2 and 3) clearly show that insertion of the diiron moiety into the sulfanyl C–S bond of the ligand occurs specifically. Coordination around both metallic centers can be

Table 1
Crystallographic Data for Compounds **3a**, **3c**, **4**, **5** and **6**

	3a	3c	4	6	5
Formula	$\text{C}_{12}\text{H}_8\text{Fe}_2\text{O}_8\text{S}_2$	$\text{C}_{18}\text{H}_{12}\text{Fe}_2\text{O}_9\text{S}_2$	$\text{C}_8\text{H}_4\text{Fe}_2\text{O}_6\text{S}_2$	$\text{C}_8\text{H}_6\text{Fe}_2\text{O}_6\text{S}_2$	$\text{C}_{17}\text{H}_{12}\text{Fe}_2\text{O}_7\text{S}_2$
Formula weight (g mol^{-1})	456.00	548.10	371.93	373.95	504.09
Crystal size (mm)	$0.42 \times 0.28 \times 0.07$	$0.308 \times 0.078 \times 0.044$	$0.338 \times 0.134 \times 0.024$	$0.276 \times 0.192 \times 0.136$	$0.358 \times 0.098 \times 0.022$
Color	Red	Orange	Red	Red	Deep red
Crystal system	Monoclinic	Monoclinic	Monoclinic	Triclinic	Monoclinic
Space group	$P2_1/c$	$P2_1/n$	$P2_1/n$	$P\bar{1}$	$P2_1/n$
a (\AA)	12.758(2)	14.339(2)	8.979(1)	8.1027(4)	12.620(1)
b (\AA)	9.206 (1)	8.490(1)	15.751 (1)	11.892(1)	11.238(1)
c (\AA)	15.346(3)	18.065(2)	9.537(1)	14.249(1)	14.575(1)
α ($^\circ$)	90	90	90	87.783(1)	90
β ($^\circ$)	107.74(1)	99.160(2)	101.633(2)	77.809(1)	110.968(2)
γ ($^\circ$)	90	90	90	81.968(1)	90
V (\AA^3)	1716.7(5)	2171.2(5)	1321.1(2)	1328.8(2)	1930.2(3)
Z	4	4	4	4	4
D_{calc} (g cm^{-3})	1.764	1.677	1.870	1.869	1.735
No. of collected reflections	2960	24,547	10,696	15,862	22,219
No. of independent reflections (R_{int})	2821(0.0493)	3843(0.173)	2323(0.0744)	4688(0.0440)	3403(0.1113)
No. of observed reflections	2821	3843	2323	4688	3403
Absorption correction method	Psi-scans	Face-indexed	Face-indexed	Face-indexed	Face-indexed
Max. and min. transmission	0.966 and 0.612	0.965 and 0.801	0.970 and 0.762	0.854 and 0.743	0.961 and 0.581
No. of parameters	218	281	163	329	254
R^a	0.048	0.055	0.052	0.030	0.062
R_w^b	0.101	0.098	0.096	0.048	0.076
GoF	1.017	1.018	0.981	0.986	1.004

$$^a R = \sum ||F_o| - |F_c|| / \sum |F_o|.$$

$$^b R_w(F_o)^2 = [\sum w(F_o^2 - F_c^2)^2 / \sum wF_o^4]^{1/2}.$$



Scheme 3.

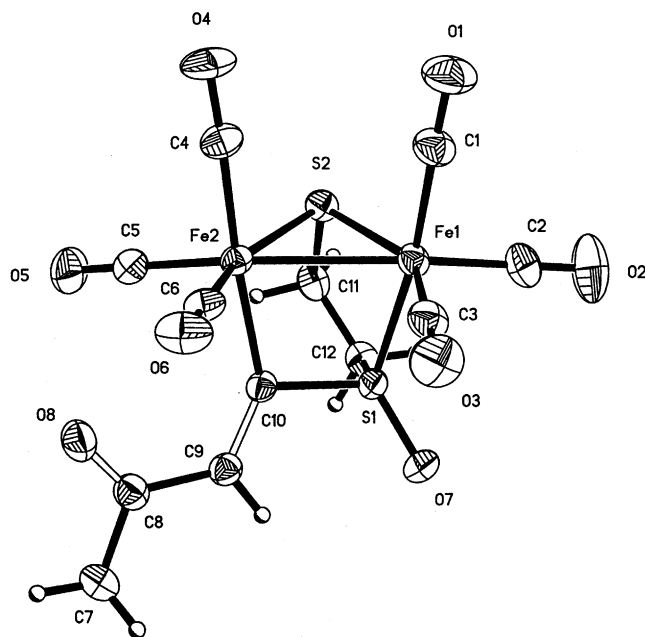


Fig. 2. ORTEP drawing of complex **3a**. Thermal ellipsoids at 30% probability level.

described as distorted octahedrons, with the μ_2 -S atom and the second iron atom occupying two of the equatorial positions, while the sulfinyl S-atom occupies the apical position in one case and the C-atom of the ylidene moiety in the other. Although the binuclear core share many features with the structure of $(\mu_2$ -ethanesulfenatothiolato- S,S')-bis(tricarbonyl)-iron reported by Messelhauser et al. [16], the moiety is less rigid, having iron-iron bond lengths and $S \cdots S$ interactions longer by ca. 0.1 and 0.2 Å, respectively. A considerable deviation from the perfect C_{2v} symmetry was also observed which cause that the perfect eclipsed bridging methylenes in the Messelhauser's structure now display a conformation intermediate between eclipsed and gauge conformations (angles $S-CH_2-CH_2-S$: 27.5° for **3a** and 25.1° for **3c**). On both cases the 3-oxo-propen-1-en-1-sulfinyl moiety

Table 2

Selected bond lengths (Å) and angles (°) for **3a**

Bond lengths			
Fe(1)–Fe(2)	2.626(1)	Fe(2)–C(5)	1.805(8)
Fe(1)–S(1)	2.183(2)	Fe(2)–C(6)	1.784(7)
Fe(1)–S(2)	2.245(2)	S(1)–C(12)	1.800(7)
Fe(2)–S(2)	2.260(2)	S(2)–C(11)	1.845(7)
Fe(1)–C(1)	1.812(8)	C(11)–C(12)	1.516(10)
Fe(1)–C(2)	1.820(8)	C(9)–C(10)	1.353(8)
Fe(1)–C(3)	1.806(8)	S(1)–O(7)	1.468(5)
Fe(2)–C(4)	1.810(7)	Fe(2)–C(10)	2.004(6)
S(1) \cdots S(2)	2.925(1)		
Bond angles			
C(1)–Fe(1)–C(2)	93.4 (4)	C(5)–Fe(2)–S(2)	101.7(2)
C(3)–Fe(1)–C(1)	91.1(3)	C(10)–Fe(2)–S(2)	93.8(2)
C(1)–Fe(1)–S(1)	172.9(3)	C(5)–Fe(2)–Fe(1)	152.1(2)
C(3)–Fe(1)–S(2)	146.8(2)	C(10)–Fe(2)–Fe(1)	79.9(2)
C(2)–Fe(1)–Fe(2)	161.8(3)	C(9)–C(10)–Fe(2)	140.8(5)
S(2)–Fe(1)–Fe(2)	54.6(5)	S(1)–Fe(1)–Fe(2)	76.0(5)
C(6)–Fe(2)–C(4)	91.0(3)	S(1)–Fe(1)–S(2)	82.7(7)
C(6)–Fe(2)–C(10)	86.4(3)	O(7)–S(1)–C(12)	103.1(3)
C(4)–Fe(2)–C(10)	174.6(3)		

display a s-syn, s-syn conformation with considerable deviation from planarity (Tables 1–3).

The compound **5** (Fig. 4) is totally analogous to [4-phenyl-1-(1,3-dithiolane-2-ylidene)-3*E*-butene-2-one] $Fe_2(CO)_5$, previously reported, [7] showing a nearly symmetrical μ -S and totally asymmetrical μ -C nature of the ligand towards the binuclear iron, as well as the σ -O and σ -S coordination as the most salient features of the structure (Tables 1 and 4).

When sulfoxide **2d** was reacted with $Fe_2(CO)_9$ under the aforementioned conditions (Scheme 4) complexes **3d** and **6** were obtained. The IR spectrum of **3d** displays bands at 2101, 2039, and 2002 cm^{-1} for M–CO. The 1H NMR data of **3d** showed signals at 2.25 and 2.76 ppm for methyl groups attached to the sulfur atom which are shifted to higher frequencies with respect to the free ligand. The ^{13}C NMR displays a similar shift towards

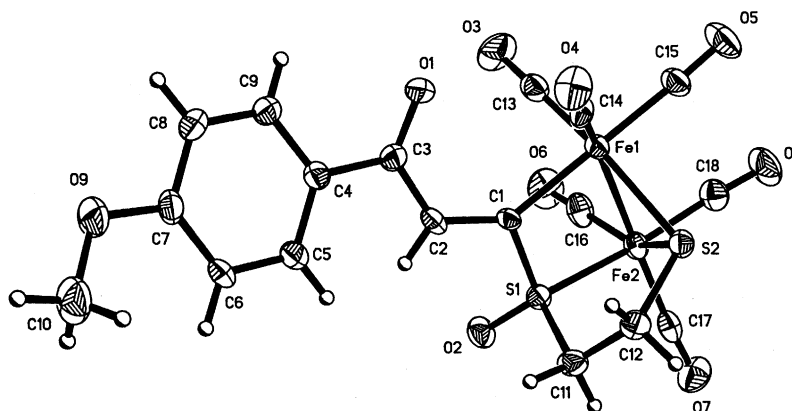


Fig. 3. ORTEP drawing of complex **3c**. Thermal ellipsoids at 30% probability level.

Table 3
Selected bond lengths (Å) and angles (°) for **3c**

<i>Bond lengths</i>			
Fe(1)–Fe(2)	2.642(1)	Fe(2)–C(16)	1.804(7)
Fe(1)–S(2)	2.252(2)	Fe(2)–C(17)	1.797(7)
Fe(2)–S(1)	2.198(1)	F2(2)–C(18)	1.797(6)
Fe(2)–S(2)	2.235(2)	S(1)–C(11)	1.795(5)
Fe(1)–C(1)	1.993(4)	S(2)–C(12)	1.832(5)
Fe(1)–C(15)	1.813(6)	C(11)–C(12)	1.522(7)
Fe(1)–C(14)	1.784(6)	C(1)–C(2)	1.359(6)
Fe(1)–C(13)	1.796(7)	S(1)–O(2)	1.473(3)
S(1)⋯S(2)	2.929(1)		
<i>Bond angles</i>			
C(14)–Fe(1)–C(13)	100.8(2)	C(17)–Fe(2)–C(16)	103.3(3)
C(14)–Fe(1)–C(15)	93.9(2)	C(18)–Fe(2)–S(1)	169.4(2)
C(13)–Fe(1)–C(15)	91.5(2)	C(17)–Fe(2)–S(1)	96.5(2)
C(14)–Fe(1)–C(1)	91.8(2)	C(16)–Fe(2)–S(1)	89.9(2)
C(14)–Fe(1)–C(1)	85.4(2)	C(18)–Fe(2)–Fe(1)	158.8(2)
C(15)–Fe(1)–C(1)	173.9(2)	C(17)–Fe(2)–Fe(1)	96.4(2)
C(14)–Fe(1)–S(2)	101.7(2)	S(1)–Fe(2)–Fe(1)	75.5(4)
C(13)–Fe(1)–S(2)	157.5(2)	S(2)–Fe(2)–Fe(1)	54.2(4)
C(1)–Fe(1)–S(2)	91.7(2)	O(2)–S(1)–C(1)	115.7(2)
C(15)–Fe(1)–S(2)	89.2(2)	O(2)–S(1)–C(11)	108.8(2)
C(14)–Fe(1)–Fe(2)	53.6(4)	C(1)–S(1)–C(11)	101.2(2)
C(18)–Fe(2)–C(17)	91.7(2)	O(2)–S(1)–Fe(2)	124.3(2)
C(18)–Fe(2)–C(16)	94.6(3)	C(1)–S(1)–Fe(2)	98.4(2)

Table 4
Selected bond lengths (Å) and angles (°) for **5**

<i>Bond lengths</i>			
Fe(1)–Fe(2)	2.624(1)	Fe(2)–C(17)	1.737(6)
Fe(1)–S(2)	2.251(2)	Fe(2)–O(1)	1.946(3)
Fe(2)–S(1)	2.326(2)	Fe(2)–C(1)	1.910(5)
Fe(2)–S(2)	2.212(2)	S(1)–C(1)	1.752(5)
Fe(1)–C(1)	2.265(5)	S(1)–C(11)	1.819(5)
Fe(1)–C(15)	1.796(7)	S(2)–C(12)	1.800(5)
Fe(1)–C(14)	1.763(7)	O(1)–C(3)	1.309(5)
Fe(1)–C(13)	1.780(8)	C(1)–C(2)	1.413(6)
Fe(2)–C(16)	1.802(6)	C(2)–C(3)	1.373(6)
<i>Bond angles</i>			
C(14)–Fe(1)–C(13)	90.6(3)	C(1)–Fe(1)–Fe(2)	45.3(1)
C(14)–Fe(1)–C(15)	101.3(3)	C(17)–Fe(2)–C(16)	99.2(3)
C(13)–Fe(1)–C(15)	97.0(3)	C(1)–Fe(1)–Fe(2)	45.3(1)
C(15)–Fe(1)–S(1)	103.5(2)	C(17)–Fe(2)–C(1)	95.4(2)
C(14)–Fe(1)–C(1)	110.1(2)	C(16)–Fe(2)–C(1)	163.9(2)
C(13)–Fe(1)–C(1)	88.0(2)	C(17)–Fe(2)–O(1)	97.8(2)
C(14)–Fe(1)–S(2)	87.5(2)	C(16)–Fe(2)–O(1)	90.4(2)
C(15)–Fe(1)–S(2)	92.9(2)	S(1)–Fe(2)–Fe(1)	82.1(4)
C(1)–Fe(1)–S(2)	83.5(1)	S(2)–Fe(2)–Fe(1)	53.3(4)
C(13)–Fe(1)–S(1)	89.9(2)	C(1)–Fe(2)–S(2)	90.1(2)
C(14)–Fe(1)–Fe(2)	75.3(2)	O(1)–Fe(2)–Fe(1)	106.5(1)
C(13)–Fe(1)–Fe(2)	116.8(2)	O(1)–Fe(2)–S(2)	159.2(1)
C(15)–Fe(2)–Fe(2)	145.9(2)	S(2)–Fe(2)–Fe(1)	54.7(1)

lower frequencies for groups OSCH₃ and CHCFeSO ($\delta = 4$ and 3), respectively. In the mass spectrum of **3d** appeared the ion $m/z = 326$ which agreed with a dinuclear complex. Likewise, the complex **6** was also isolated as red crystals in 20% yield [17], and then its structure was established by X-ray diffraction. This compound crystallized with two molecules chemically identical but crystallographic independent showing the presence of a Fe₂S₂ core in a butterfly form and possessing an approximately C_{2v} molecular symmetry with the methyl groups of the bridging sulfur atoms in a *syn-endo* position, as can be seen from Fig. 5. The Fe–Fe bonds and the S⋯S separations are consistent with the comparable distances in related compounds (Table 6).

3. Conclusion

The noteworthy feature is the fact that the presence of a sulfoxide group implies a different reactivity at the formation of the dinuclear Fe(0) complex. Thus, the reaction between the ligands **2a** or **2c** and Fe₂(CO)₉ leads to the formation of the new dinuclear complexes **3a** and **3c**. The X-ray diffraction study showed that both metallic centers Fe1 and Fe2 are surrounded by three terminal carbonyl groups whereas, the complex **5** displays a different coordination pattern. The Fe2 atom is surrounded by two terminal carbonyl groups while Fe1 atom by three terminal carbonyl groups. The coordination of Fe2 is accomplished by a σ -O bond from the

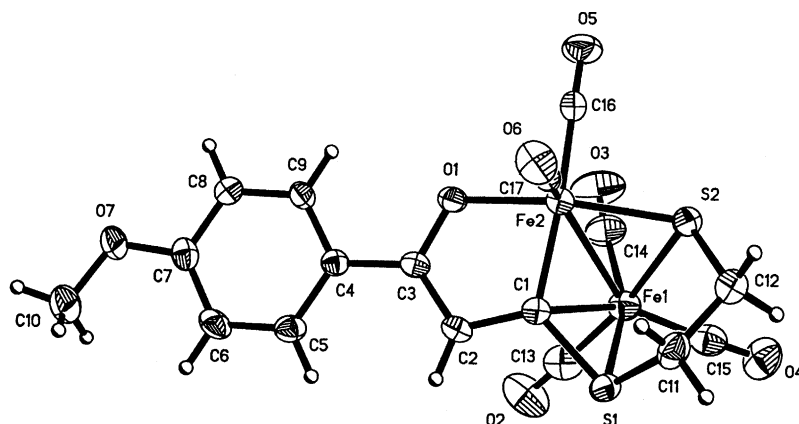
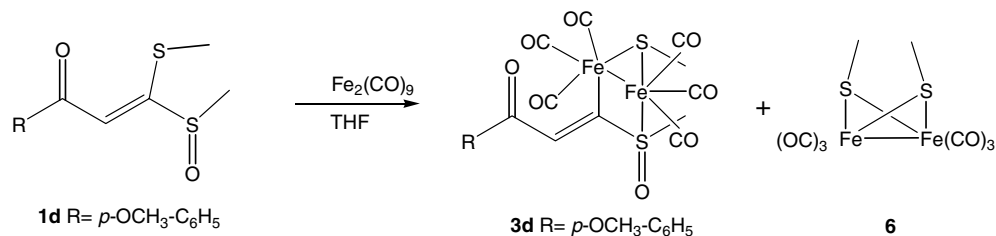
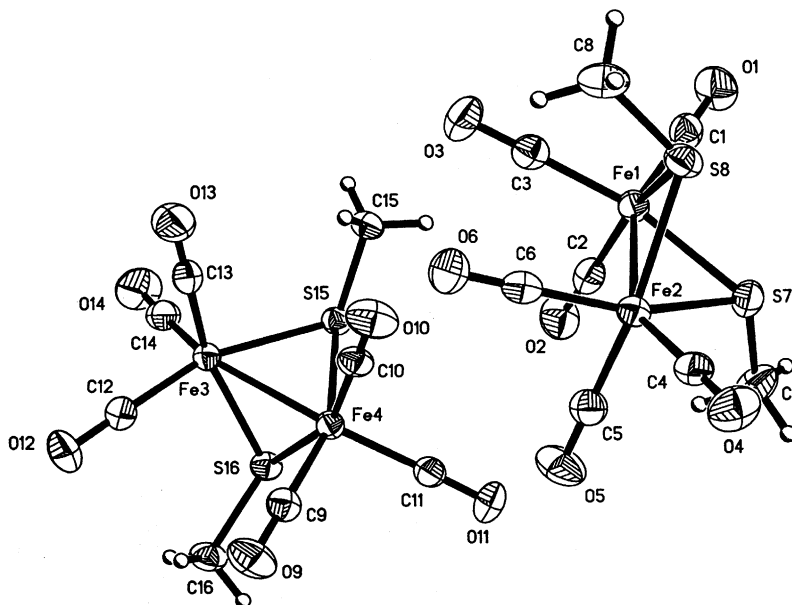


Fig. 4. ORTEP drawing of complex **5**. Thermal ellipsoids at 30% probability level.



Scheme 4.

Fig. 5. ORTEP drawing of complex **6**. Thermal ellipsoids at 30% probability level.

ketone oxygen atom and by a σ -S bond of the dithiolane ring. In addition, the complex **5** was found to play a role as intermediate in the reductive reaction of sulfoxide group and in the formation of complexes **4** and **6**.

4. Experimental

4.1. General methods

¹H NMR and ¹³C NMR spectra were recorded on a JEOL 300 spectrometer, using CDCl₃ as solvent and TMS as internal reference. IR spectra were performed on a Perkin–Elmer 283 B or 1420 spectrometer. The FAB spectra were obtained on a JEOL JMS SX 102A mass spectrometer operated at an accelerating voltage of 10 kV. Samples were desorbed from a nitrobenzyl alcohol matrix using a 6 keV Xenon atoms. The electronic impact (EI) ionization mass spectra were acquired on a JEOL JMS-AX505 HA Mass spectrometer operated in the positive ion mode. The acquisition conditions were ion source temperature 230 °C, ionization energy 70 eV, emission current 0.14 μ A and ionization current 100 μ A.

Mass measurements in FAB are performed at 10,000 resolution using electrical field scans and the polyethylene glycol ions as reference material. Melting points were measured using a Mel-Temp II apparatus and are uncorrected. All reagents were obtained from commercial suppliers and used as received. Reactions were performed under nitrogen atmosphere in carefully dried glassware. THF was distilled from sodium-benzophenone under argon or nitrogen atmosphere. Column chromatography was performed with Merck silica gel (70–230 mesh) using ethyl acetate:hexane in different ratios as eluent.

4.2. Synthesis of ligands

A solution of 1-(1,3-dithiolane-2-yliden) acetone derivatives [9] (0.005 mol) or 1,1-dimethylmercapto-3(4-methoxyphenyl)-1-propen-3-one [10] in methanol with sodium periodate (0.007 mol) was stirred for 72 h at room temperature. The solvent was evaporated, then, AcOEt and water (3 \times 40 ml) were also added, extracting the organic phase, drying with Na₂SO₄ and removing the volatile in vacuo. The reaction mixture was

purified by column chromatography on alumina, using hexane/AcOEt as eluent.

Ligand 1-(1-oxo-1,3-dithiolan-2-yliden)acetone **2a**, yellow solid, 28% yield, m.p.: 95 °C; IR ν_{\max} (CHCl₃) cm^{-1} = 1668.47 (CO); 1535.54 (C=C); 1049.48 (S=O) ¹H NMR (300 MHz, CDCl₃): 2.35 (s, 3H, CH₃); 3.23 (m, 2H, CH₂CS); 3.70 (m, 2H, CH₂CSO); 7.05 (s, 1H, CH-CO) ppm. ¹³C NMR (75 MHz, CDCl₃): 30.4 (CH₃); 31.7 (SCH₂); 52.9 (OSCH₂); 121.5 (HCCSSO); 164.08 (CSSO); 195.2 (CO) ppm. MS-EI (70 eV) m/z (%): 176 (M⁺)(30), 43(100).

Ligand 1-(1-oxo-1,3-dithiolan-2-yliden)acetophenone **2b** yellow solid, 39% yield, m.p.: 133–135 °C; IR ν_{\max} (CHCl₃) cm^{-1} = 1637.1 (C=O), 1529.3 (C=C), 1043.1 (S=O), 938.1 (C=C). NMR ¹H (300 MHz, CDCl₃): 3.11 (1H, m, CH₂), 3.4 (1H, m, CH₂), 3.54 (1H, s, CH₂), 3.8 (1H, m, CH₂), 7.4 (2H, t, J = 7.7 Hz, H-*m*), 7.55 (1H, t, J = 7.6 Hz, H-*p*), 7.8 (1H, s, CHCSSO), 7.9 (2H, dd, J = 7.14, 1.38 Hz, H-*o*) ppm. NMR ¹³C (75 MHz, CDCl₃): 31.7 (SCH₂), 52.9 (OSCH₂), 118.2 (CHCSSO), 128.3 (CH_m), 128.9 (CH_o), 133.4 (CH_p), 137.1 (C_i), 166.7 (CSSO), 187.6 (CO) ppm; MS-EI (70 eV) m/z (%): 238 [M⁺](18), 222(10), 194(10), 163(1), 105(100), 77(40).

Ligand 1-(1-Oxo-1,3-dithiolan-2-yliden)-*p*-methoxyacetophenone **2c** yellow solid, 35% yield, m.p.: 134–135 °C; IR (sol. CHCl₃) ν_{\max} : 1634.5 (C=O), 1599.8 (C=C), 1043.0 (S=O) cm^{-1} . NMR ¹H (300 MHz, CDCl₃): 3.08–3.11(1H, m, CH₂), 3.39–3.43 (1H, m, CH₂), 3.52–3.56 (1H, m, CH₂), 3.85–3.87 (1H, m, CH₂), 3.86 (3H, s, CH₃), 6.95 y 7.99 (4H, AA'BB', J = 7.0 Hz, H-*o*, H-*m*), 7.78 (1H, s, CHCSSO) ppm. NMR ¹³C (75 MHz, CDCl₃): 31.6 (SCH₂), 52.9 (OSCH₂), 55.6 (CH₃-O), 114.2 (CHCSSO), 118.4 (CH_m), 130.1 (C_i-CO), 130.7 (CH_o), 163.8 (C_i-OMe), 165.5 (CSSO), 186.1 (CO) ppm; MS-EI (70 eV) m/z (%): 268 [M⁺](10), 252(3), 240(15), 224(4), 208(5), 192(1), 177(1), 135(100), 107(8), 92(13), 77(14).

Ligand 3-methylmercapto-3'-oxomethylmercapto-1-(*p*-methoxyphenyl)-2-propen-1-one **2d** yellow solid, 27% yield, m.p.: 144–150 °C; IR (sol. CHCl₃) ν_{\max} : 1172.1 (C=O), 1048.7 (S=O), 929.1 (C=C) cm^{-1} . NMR ¹H (300 MHz, CDCl₃): 2.47 (3H, s, CH₃), 2.98 (3H, s, CH₃), 3.85 (3H, s, CH₃), 6.84 (1H, s, CHCSSO), 6.9 y 7.9 (4H, AA'BB', J = 8.5 Hz, H-*o*, H-*m*) ppm. NMR ¹³C (75 MHz, CDCl₃): 15.8 (SCH₃), 43.9 (OSCH₃), 55.6 (OCH₃), 114.1 (CH_m), 114.4 (CHCSSO), 130.0 (C_i-CO), 130.9 (CH_o), 163.8 (C_i-OMe), 178.9 (CSSO), 184.2 (CO) ppm. MS-EI (70 eV) m/z (%): 270 [M⁺](1), 255(1), 239(2), 207(14), 193(2), 163(0.5), 135(100), 107(9), 77(11).

4.3. Synthesis of complexes

A solution of the ligand **2a–2d** (1 mmol) in anhydrous THF (40 ml) was treated with Fe₂(CO)₉ (3 mmol) with magnetic stirring at room temperature for 24 h under inert atmosphere. After the reaction was complete, the

crude was filtered off through an alumina column and the solvent was evaporated under vacuum. The reaction mixture was chromatographed on silica gel and elution with hexane/ethyl acetate in different ratio gave the corresponding Fe(0) complexes. The yields were based on the pure products isolated.

Complex 3,3,3,7,7,7-hexacarbonyl-1-oxo-2-(2-oxo-propyliden)-3,7-diferra-1,4-dithiatricycle[2.2.1.1^{3,4}]heptane **3a** as red crystals, 14% yield, m.p.: 83 °C; IR ν_{\max} (sol. CHCl₃) cm^{-1} : 2022, 2047, 2084 (M-CO). ¹H NMR (300 MHz, CDCl₃): 2.34 (s, 3H, CH₃); 3.58–2.62 (m, 4H, SCH₂CH₂Fe); 7.35 (s, 1H, CHCFeSO); ppm. ¹³C NMR (75 MHz, CDCl₃): 26.9 (FeSCH₂); 29.9 (CH₃); 32.9 (OSCH₂); 135.4 (CHCFeSO); 167.9 (CFeSO); 190.8 (CO); 206.6 (M-CO) ppm MS-EI (70 eV) m/z (%): 428 (M⁺ - CO)(20); 400 (M⁺ - 2CO)(55); 372 (M⁺ - 3CO)(25). HR-MS (FAB⁺) C₁₁H₈O₇S₂Fe₂: Found, 427.8404; Calc., 427.8412.

Complex 3,3,3,7,7,7-hexacarbonyl-1-oxo-2-(2-oxo-2-phenyletyliden)-3,7-diferra-1,4-dithiatricycle[2.2.1.1^{3,4}]heptane **3b** as red crystals 12% yield, m.p.: 150 °C (dec.); IR (sol. CHCl₃) ν_{\max} : 2922.3 (C-H), 2084.1, 2047.9, 2022.3 (M-C=O), 1015.3 (S=O), 928.3 (C=C) cm^{-1} . NMR ¹H (300 MHz, CDCl₃): 3.21–3.28 (1H, m, CH₂), 3.30–3.36 (1H, m, CH₂), 3.38–3.46(1H, m, CH₂), 3.61–3.64 (1H, m, CH₂), 7.44–7.49 (2H, m, H-*oy* H-*m*), 7.98 (1H, t, d, J = 10.3 Hz, H-*7*), 8.15 (1H, s, CHCFeSO) ppm. NMR ¹³C (75 MHz, CDCl₃): 31.56 (SCH₂), 67.68 (OSCH₂), 111.0 (CHCFeSO), 128.39 (CH_m), 128.78 (CH_o), 131.78 (CH_p), 133.17 (C_i), 179.89 (CFeSO), 188.81 (CO), 205.38, 206.43, 209.45 (M-C=O) ppm. MS-EI (70 eV) m/z (%): 490 [M⁺ - CO](5), 462(40), 434(40), 406(40), 378(35), 350(85), 322(82), 290(13), 222(12), 192(5), 176(40), 105(100), 77(62). HR-MS (FAB⁺) C₁₇H₁₁O₈S₂Fe₂: Found, 518.8587; Calc., 518.8594.

Complex 2-[2-oxo-2-(*p*-methoxyphenyl)etyliden]-3,3,3,7,7,7-hexacarbonyl-1-oxo-3,7-diferra-1,4-dithiatricycle[2.2.1.1^{3,4}]heptane **3c** as orange crystals 15% yield, m.p.: 142 °C (dec). IR ν_{\max} (KBr)/ cm^{-1} : 2081.5, 2045, 2017.7 (M-C=O), 1173.2 (S=O). NMR ¹H (300 MHz, CDCl₃): 3.17–3.20 (1H, m, CH₂), 3.35–3.42 (1H, m, CH₂), 3.43–3.45 (1H, m, CH₂), 3.61–3.65 (1H, m, CH₂), 3.86 (3H, s, CH₃), 6.93 and 7–98 (4H, AA'BB', J = 8.9 Hz, H-*o*, H-*m*), 8.12 (1H, s, CHCFeSO) ppm. NMR ¹³C (75 MHz, CDCl₃): 27.1 (SCH₂), 55.6 (OCH₃), 67.8 (OSCH₂), 113.9 (CH_m), 114.2 (CHCFeSO), 130.8 (CH_o), 132.0 (C_i-CO), 163.7 (C_i-OMe), 178.1 (CFeSO), 187.9 (CO), 205.0, 207.26, 210.81 (M-C=O) ppm. MS-EI (70 eV) m/z (%): 492 [M⁺ - 2CO](5), 464(6), 436(5), 408(5), 380(14), 352(16), 336(3), 308(4), 284(10), 252(10), 224(7), 135(100), 107(8), 92(17), 77(20). HR-MS (FAB⁺) C₁₆H₁₂O₇S₂Fe₂: Found, 491.8714; Calc., 491.8723.

Complex 6,6,10,10,10-pentacarbonyl-8-(*p*-methoxyphenyl)-6,10-diferra-7-oxa-2,5-dithiapentacycle[4.3.0.1^{2,5}.0^{1,10}.0^{6,10}]decan-7,9-diene **5** as deep red crystals, 3%

yield, m.p.: 108 °C (dec); IR (sol. CHCl₃) ν_{\max} : 2057.9, 2018.9, 1961 (M–C=O), 1602.7 (CO) cm⁻¹. NMR ¹H (300 MHz, CDCl₃): 2.05–2.25, 3.46–3.51 (3H, 1H m, CH₂–CH₂), 3.82 (3H, s, CH₃), 6.87 and 7.77 (4H, AA'BB', *J* = 8.8 Hz, H-*o*, H-*m*), 7.45 (1H, s, CHCFeSO) ppm. NMR ¹³C (75 MHz, CDCl₃): 31.0 (SCH₂), 36.24 (SCH₂), 55.4 (CH₃O), 113.7 (CH_m), 118.6 (CHCFeSO), 128.7 (CH_o), 129.7 (C_i–CO), 161.0 (C_i–OMe), 189.8 (CFeSO), 191.1 (CO), 211.3, 213.2 (M–C=O) ppm MS-FAB⁺ (70 eV) *m/z* (%): 505 [M⁺ + 1] (13), 397 (16), 307 (30), 107 (20), 77 (19). HR-MS (FAB⁺) C₁₅H₁₂O₅S₂Fe₂: Found, 447.8823; Calc., 447.8825.

Complex 4-[2-oxo-2-(*p*-methoxyphenyl)]etylidene-2,2,3,3,3-hexacarbonyl-1-methyl-3-methylmercapto-1-oxo-2,3-diferra-1-thiacyclebutane **3d** as red oil 12% yield; IR (CHCl₃) ν_{\max} : 3003.9 (C–H), 2101.3, 2039, 2002.3 (M–C=O), 1599.8 (CO), 1026.3 (S=O), cm⁻¹. NMR ¹H (300 MHz, CDCl₃): 2.25 (3H, s, CH₃), 2.76 (3H, s, CH₃), 3.86 (3H, s, CH₃), 7.29 (1H, s, CHCFeSO), 6.95 and 7.94 (4H, *J* = 7.9 Hz, AA'BB') ppm. NMR ¹³C (75 MHz, CDCl₃): 15.0 (SCH₃), 47.7 (OSCH₃), 55.6 (OCH₃), 113.8 (CH_m), 117.6 (CHCFeSO), 129.9 (C_i–CO), 130.6 (CH_o), 163.7 (C_i–OMe), 186.0 (CFeSO), 194.4 (CO), 202.2, 205.4, 207.5 (M–C=O) ppm. MS-EI (70 eV) *m/z* (%): 326 [M⁺ – Fe(CO)₆] (9), 254(8), 239(17), 193(70), 135(100), 105(10), 77(20). HR-MS (FAB⁺) C₁₂H₁₄O₃S₂Fe: Found, 325.9720; Calc., 325.9734.

4.4. X-ray crystal structure determinations of compounds **3a**, **3c**, **4**, **5** and **6**

Data collection and refinement parameters are summarized in Table 1. The diffraction data for **3a** was collected on a Siemens P4/PC diffractometer, while those of **3c**, **4**, **5** and **6** were collected on a Bruker Smart Apex CCD diffractometer with Mo K α radiation, λ = 0.71063 Å. Each data set was corrected for Lorentz and polarization effects and empirical absorption corrections based on psi-scans were applied. The structures were solved by direct methods [18] and each structure was

Table 6

Selected bond lengths (Å) and angles (°) for **6**

Bond lengths			
Fe(1)–C(3)	1.780(3)	S(7)···S(8)	2.744(1)
Fe(1)–C(2)	1.782(4)	Fe(3)–S(15)	2.266(1)
Fe(1)–C(1)	1.804(4)	Fe(3)–S(16)	2.269(1)
Fe(1)–S(7)	2.262(1)	Fe(3)–Fe(4)	2.522(1)
Fe(1)–S(8)	2.268(1)	Fe(4)–C(9)	1.777(3)
Fe(1)–Fe(2)	2.511(1)	Fe(4)–C(10)	1.784(3)
Fe(2)–C(5)	1.785(4)	Fe(4)–C(11)	1.814(3)
Fe(2)–C(6)	1.792(4)	Fe(4)–S(16)	2.259(1)
Fe(2)–C(4)	1.807(3)	Fe(4)–S(15)	2.266(1)
Fe(2)–S(7)	2.260(1)	S(15)···S(16)	2.773(1)
Fe(2)–S(8)	2.271(1)		
Bond angles			
S(7)–Fe(1)–S(8)	74.56(3)	S(15)–Fe(3)–S(16)	75.40(3)
S(7)–Fe(1)–Fe(2)	56.24(2)	S(15)–Fe(3)–Fe(4)	56.18(2)
S(8)–Fe(1)–Fe(2)	56.48(2)	S(16)–Fe(3)–Fe(4)	55.96(2)
S(7)–Fe(2)–S(8)	74.53(3)	S(16)–Fe(4)–S(15)	75.60(3)
S(7)–Fe(2)–Fe(1)	56.31(2)	S(16)–Fe(4)–Fe(3)	56.34(2)
S(8)–Fe(2)–Fe(1)	56.36(2)	S(15)–Fe(4)–Fe(3)	56.19(2)
Fe(2)–S(7)–Fe(1)	67.45(3)	Fe(4)–S(15)–Fe(3)	67.63(3)
Fe(1)–S(8)–Fe(2)	67.16(3)	Fe(4)–S(16)–Fe(3)	67.70(3)

refined by full-matrix least squares on F^2 using all data with the all non-hydrogen atoms assigned anisotropic displacement parameters and hydrogen atoms bound to carbon atoms inserted at calculated position with isotropic temperature factor 1.2 times the U_{iso} of the parent carbon atom. The program used in the final refinements was SHELXL 97 [19]. Selected bond lengths and bond angles are shown in Tables 2–6.

5. Supplementary data

Crystallographic data or the structural analysis has been deposited with the Cambridge Crystallographic Centre CCDC No.220305 for complex **3a**, No. 220306 for complex **3c**, No. 220307 for complex **4**, No. 220308 for complex **6** and No. 220309 for complex **5**. Copies of this information may be obtained free of charge from The Director, 12 Union Road, Cambridge, CB2 1EZ, UK (fax: +44 1223 336033; e-mail: deposit@ccdc.cam.ac.uk or [www: http://www.ccdc.cam.ac.uk](http://www.ccdc.cam.ac.uk)).

Acknowledgements

We thank DGAPA for financial support (Project # IN216201). The technical assistance of Rocio Patiño, Luis Velasco and Javier Pérez is gratefully acknowledged.

References

- [1] C. Alvarez-Toledano, A.C. Cano, R.A. Toscano, A. Parlier, H. Rudler, Bull. Soc. Chim. Fr. 130 (1993) 601.
- [2] N.W. Alcock, C.J. Richards, S.E. Thomas, Organometallics 10 (1991) 231.

Table 5

Selected bond lengths (Å) and angles (°) for **4**

Bond lengths			
Fe(1)–C(1)	1.774(8)	Fe(2)–C(6)	1.800(8)
Fe(1)–C(3)	1.788(8)	Fe(2)–C(5)	1.805(7)
Fe(1)–C(2)	1.813(7)	Fe(2)–S(1)	2.240(2)
Fe(1)–S(1)	2.236(2)	Fe(2)–S(2)	2.242(2)
Fe(1)–S(2)	2.238(2)	S(1)–C(7)	1.806(7)
Fe(1)–Fe(2)	2.505(2)	S(2)–C(8)	1.820(7)
Fe(2)–C(4)	1.787(8)		
Bond angles			
S(1)–Fe(1)–S(2)	80.54(7)	S(1)–Fe(2)–Fe(1)	55.91(5)
S(1)–Fe(1)–Fe(2)	56.03(5)	S(2)–Fe(2)–Fe(1)	55.93(5)
S(2)–Fe(1)–Fe(2)	56.08(5)	Fe(1)–S(1)–Fe(2)	68.06(6)
S(1)–Fe(2)–S(2)	80.39(7)	Fe(1)–S(2)–Fe(2)	67.99(5)

- [3] T.A. Mitsudo, H. Watanabe, T. Sasaki, Y. Takegami, Y. Watanabe, K. Kafuku, K. Nakatsu, *Organometallics* 8 (1989) 368, and references cited therein.
- [4] J. Klimes, E. Weiss, *Angew. Chem. Int. Ed. Engl.* 21 (1982) 205.
- [5] C. Alvarez, R. Gutiérrez, R.A. Toscano, M. Moya, L. Velasco, R. Rosas, R. Tapia, G. Penieres, *J. Coord. Chem.* 48 (1999) 383.
- [6] C. Alvarez-Toledano, J. Enríquez, R.A. Toscano, M. Martínez-García, E. Cortés-Cortés, Y. Osornio, O. García, R. Gutiérrez-Pérez, *J. Organomet. Chem.* 577 (1999) 38.
- [7] F. Ortega-Jiménez, M.C. Ortega-Alfaro, J.G. López-Cortés, R. Gutiérrez-Pérez, R.A. Toscano, L. Velasco-Ibarra, E. Peña-Cabrera, C. Alvarez-Toledano, *Organometallics* 19 (2000) 4127.
- [8] C. Alvarez-Toledano, R. Gutiérrez-Pérez, R.A. Toscano, M. Moya-Cabrera, T. Haquet, M.C. Ortega, A. Cabrera, *Polyhedron* 20 (2002) 215.
- [9] (a) A. Thullier, J. Viallé, *Bull. Soc. Chim. Fr.* (1959) 1398;
(b) F.C.V. Larsson, S.O. Lawesson, *Tetrahedron* 28 (1972) 5341.
- [10] (a) I. Shihak, Y. Sasson, *Tetrahedron Lett.* (1973) 4207;
(b) K.T. Potts, M.J. Cipullo, P. Ralli, G. Theodoridis, *J. Org. Chem.* 47 (1982) 3027.
- [11] (a) P. Sykes, A.R. Todd, Committee on Penicillin Synthesis Report 526, 677;
(b) N.J. Leonard, C.R. Johnson, *J. Org. Chem.* 27 (1962) 282.
- [12] P. Yates, T.R. Lunch, D.R. Moore, *Can. J. Chem.* 49 (1971) 1467.
- [13] A. Shawer, P.J. Fitzpatrick, K. Steliow, I.S. Butter, *J. Am. Chem. Soc.* 101 (1979) 1313.
- [14] (a) D.L. Hughes, G.L. Leigh, D.R. Paulson, *Inorg. Chim. Acta* 120 (1986) 191;
(b) F. Dahl, C.H. Suan, *Inorg. Chem.* 4 (1965) 1.
- [15] D.F. Shriver, K.H. Whitmire, *Comprehensive Organometallic Chemistry*, in: G. Wilkinson, F.G. Stone, E.W. Abel (Eds.), *The Synthesis, Reactions and Structures of Organometallic Compounds*, vol. 4, Pergamon Press, Oxford, 1982, pp. 251–252.
- [16] J. Messelhauser, K.U. Gutensohn, I.P. Lorenz, W. Hiler, *J. Organomet. Chem.* 321 (1987) 377.
- [17] L.F. Dahl, C.H. Wei, *Inorg. Chem.* 2 (1963) 328.
- [18] A. Altomare, G. Cascarano, C. Giacovazzo, A. Guagliardi, M.C. Burla, G. Polidori, M. Canalli, *J. Appl. Cryst.* 27 (1994) 435.
- [19] G.M. Sheldrick, SHELXL 97 Program for refinement of crystal structures, University of Goettingen, Germany.